sults prior to publication.

[7]F. D. Feiock and W. R. Johnson, Phys. Rev. 187, 39 (1969).

[8]Data and citation of published material will be found in Raghavan *et al.*, Ref. 6. Unpublished data for $Be^{181}Ta$ (interstitial) is from E. N. Kaufmann, K. Krien, J. C. Soares, and K. Freitag, private communication, and to be published.

[9]K. W. Lodge and C. A. Scholl, J. Phys. F: Metal Phys. 4, 2073 (1974).

# Direct Nonvertical Interband and Intraband Transitions in Al

E. Petri

*Sektion Physik, Universität München, München, Federal Republic of Germany*

and

A. Otto

*Max-Planck-Institut für Festkörperforschung, Stuttgart, Federal Republic of Germany*

(Received 3 March 1975)

Electron-energy-loss spectra of epitaxial Al foils of {110} orientation show previously unobserved structures between 1.5 and 10 eV for the momentum transfer $\vec{k}$ in directions ⟨100⟩, ⟨110⟩, and ⟨111⟩. For $\vec{k} \parallel \langle 100 \rangle$, this structure may be consistently interpreted within the essential features of the nearly-free-electron-band structure. Interband transitions show a marked influence on the plasmon dispersion for small $k$; only for $k > 0.75$ Å$^{-1}$ may it be discussed within the jellium model.

Important information on the electronic structure of crystalline solids is contained in the dielectric response function $R = [\hat{k}\vec{\epsilon}(\omega\vec{k})\hat{k}]^{-1}$, where $\vec{\epsilon}(\omega\vec{k})$ is the macroscopic dielectric tensor for the macroscopic fields of phase $\exp[i(\vec{k}\cdot\vec{x} - \omega t)]$. The electron-energy-loss cross section with electrons of some 10 keV kinetic energy is given by[1]

$$(e/\pi\hbar v)^2(1/k^2)\,\mathrm{Im}R.$$

For a free degenerate electron gas Im$R$ contains a strong plasmon peak for values lower than the classical plasmon cutoff $k_c \sim \omega_p/V_F{}^2$ and weak structures at lower energies due to single-particle excitations.[3] These structures have as yet only been observed by Raman scattering from degenerate semiconductor plasmas.[4] For a nearly-free-electron metal like aluminum, one should expect an influence of the crystalline background of the atomic cores both on the spectrum of the single-particle excitations and on the dispersion of the plasmons.

Here we report electron-energy-loss spectra from Al films of {110} orientation, which were epitaxially grown by vapor deposition on polished {110} faces of rock salt.[5] The experimental procedure has been described elsewhere.[6] Energy-loss spectra were monitored for $\vec{k}$ in the ⟨100⟩ (see Fig. 1), ⟨110⟩, and ⟨111⟩ directions. For $\vec{k} \approx 0$ one observes the surface plasmon at the Al-aluminium-oxide interface at about 6.5 eV.[7] It disappears for $k$ not far from zero, because its theoretical cross section decreases as $k^{-3}$.[8] For $k > 0.3$ Å$^{-1}$, new structures appear whose dispersion and shape are different for the different crystalline directions. For $\vec{k} \parallel \langle 100 \rangle$, two separate peaks become apparent in the spectra. The dispersion of these structures is plotted in Fig. 2.

We assign them to direct nonvertical interband and intraband transitions, which correspond to the low-energy single-particle excitations in a free-electron gas, mentioned above. The structures for $\vec{k} \parallel \langle 100 \rangle$ may be explained qualitatively in the following way: The pseudopotential $U_{200}$ splits the free-electron parabolic band at the Brillouin-zone boundaries of class {100} into parallel bands of $2U_{200} = 1.5$ eV distance. Optical (vertical) interband transitions between these parallel bands (so-called parallel-band transitions[9]) occur mainly near the $W$ points and the $X$-$W$-$X$ direction in the extended-zone scheme.[10] This transition at 1.5 eV is found experimentally in $\epsilon_2(\omega, 0)$, superimposed on the Drude-type susceptibility of free electrons.[11,12] For $\vec{k} \parallel \langle 100 \rangle$, $\vec{k}$ is parallel to $X$-$W$-$X$ on four {100} zone boundaries and parallel to $X$-$\Gamma$-$X$ on two {100} zone boundaries. Therefore, the main effect may be explained by help of these two orientations. A quantitative analysis has to consider transitions throughout the Brillouin zone and $\vec{k}$-dependent

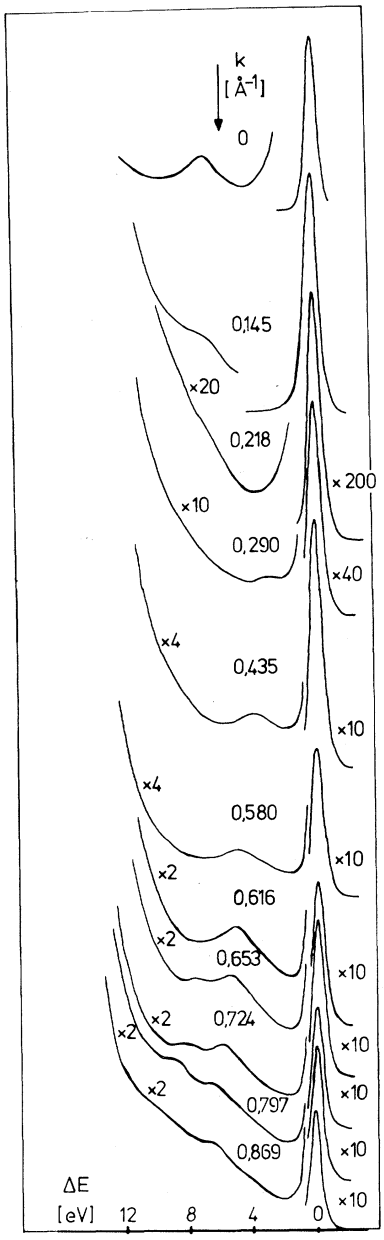


FIG. 1. Energy-loss spectra in an epitaxial foil of (100) orientation of about 700 Å thickness, for $\vec{k}$ in the ⟨100⟩ direction. Energy resolution 0.7 eV.

matrix elements. Calculations of this type have only been done without local-field corrections,[13] but should also be possible with local-field corrections (see Louie, Chelikowsky, and Cohen[14] and references there). Our qualitative argument follows from Fig. 3, where we have plotted the essential features of the band structure of Al for the line $X$-$\Gamma$-$X$ and $X$-$W$-$X$ in the extended-zone scheme, omitting all details. The joint density

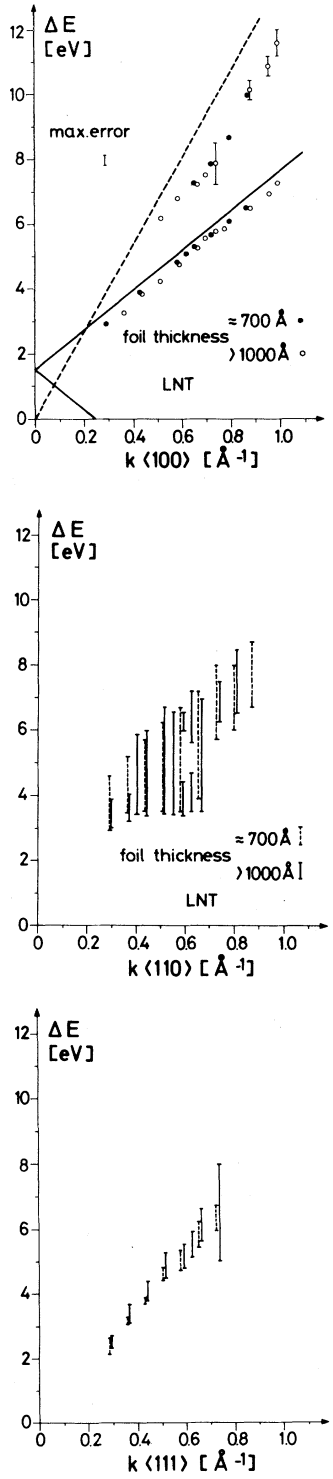


FIG. 2. Dispersion of the energy-loss structures for $\vec{k}$ in the ⟨100⟩, ⟨110⟩, and ⟨111⟩ directions. Solid line: nonvertical interband transitions; dashed line: nonvertical intraband transitions, from the nearly-free-electron model in Fig. 3.

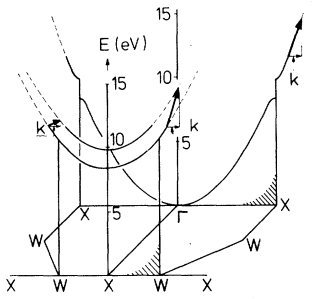


FIG. 3. Direct interband transitions in a nearly-free-electron-band scheme of Al for the $X$-$\Gamma$-$X$ and $W$-$X$-$W$ lines in the extended-zone scheme, in a perspective view. Three nonvertical direct transitions for given $k$ in the ⟨100⟩ direction are indicated.

of states for nonvertical transitions parallel to the direction of $\vec{k}$ in Fig. 3 has its maximum along these two lines. Electrons at the Fermi surface have energy transitions $\Delta E$, which are linear in $\vec{k}$ for small $\vec{k}$:

$$\Delta E = (\hbar^2 k_F/m)k$$

on line $X$-$\Gamma$-$X$ and

$$\Delta E = 2U_{200} \pm \frac{\hbar^2}{m}\left[k_F^2 - \left(\frac{2\pi}{a}\right)^2\right]^{1/2} k$$

on line $X$-$W$-$X$ ($a$ is the cubic-lattice constant). These relations are plotted in Fig. 2. The experimental points are lower than the theoretical lines, probably because nonvertical transitions also start below the Fermi surface, where $\Delta E$ is smaller for given $\vec{k}$. The transition at 1.5 eV for $\vec{k} \approx 0$ has been observed with 0.2 eV resolution by using a Wien filter,[15] thereby reproducing earlier measurements.[16]

The structures due to nonvertical interband transitions show an analogy to the so-called zone-boundary collective mode, postulated by Foo and Hopfield.[17] This mode is a nonvertical interband transition in alkali metals to the split final states at the first-Brillouin-zone edge. The Al-ion cores have an influence on the dispersion of the bulk plasmon.[6] Kloos[18] and the authors in Ref. 6 found a different dispersion of the plasmon below and above $k = 0.75$ Å$^{-1}$ for polycrystalline Al. For $k < 1.5$ Å$^{-1}$ this dispersion is plotted in Fig. 4. For $k > 0.75$ Å$^{-1}$, the dispersion is well described by

$$\omega = \omega_p + \alpha(\hbar/m)k^2,$$

with $\alpha = 0.401 \pm 0.007$ and $\hbar\omega_p = 14.5 \pm 0.15$ eV, and

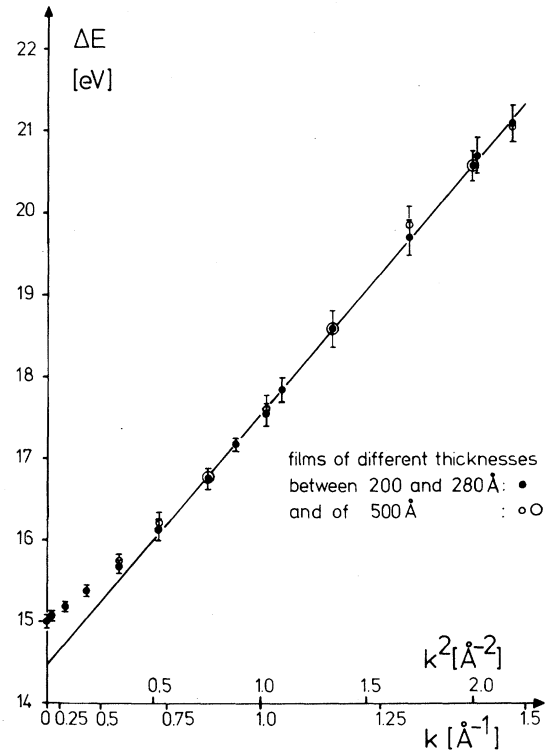


FIG. 4. Plasmon dispersion in polycrystalline Al foils for $k < 1.5$ Å$^{-1}$.

may be discussed within the framework of the jellium model.

The theoretical value of $\alpha$ within the random-phase approximation with exchange corrections[19] is

$$\alpha_{RPA} = \frac{3E_F}{5\hbar\omega_p}\left(1 - \frac{\hbar^2\omega_p^2}{16E_F^2}\right)$$

which yields $\alpha \approx 0.393$ for Al without background polarizability. With the local field corrections of Vashishta and Singwi[20] $\alpha$ is given by

$$\alpha_{VS} = \frac{3E_F}{5\hbar\omega_p}\left(1 - \frac{5}{12}\gamma\frac{\hbar^2\omega_p^2}{E_F^2}\right)$$

which yields, with the values tabulated in Ref. 20,

$$\alpha_{VS} \approx 0.355.$$

It remains an open question why the random-phase-approximation value shows better agreement with experiment (although the random-phase approximation yields an unphysical negative electron pair correlation at short distances) than the Vashishta-Singwi value (where this inconsistency has been removed from the theory). Below $k \approx 0.75$ Å$^{-1}$, there is a different dispersion, prob-

ably caused by the interband transition due to the pseudopotentials $U_{111}$ and $U_{200}$ with vertical transitions at 0.4 and 1.5 eV.[21] The influence of the band splitting and the relative difference between interband and intraband transitions become less when the energy transfer to an electron exceeds the band splittings. Therefore, it is expected that the plasmon dispersion will eventually, for increasing $k$, be well described within the jellium model—as is indeed the case. When $k$ increases further and equals a Brillouin-zone-boundary vector, there is the theoretical possibility of the splitting of the plasmon dispersion curve and the formation of plasmon bands.[22,23] Our measurements[24] did not unravel this effect. For still greater $k$, the short-range correlation between the electrons influences the dispersion of the plasmon.[6,25]

We thank J. Höhberger for valuable assistance and discussions, H. Lamvan for the preparation of the epitaxial Al films, and M. Cardona for a discussion.

[1]J. Hubbard, Proc. Phys. Soc., London, Sect. A 68, 976 (1955).
[2]R. A. Ferrell, Phys. Rev. 107, 450 (1957).
[3]K. L. Kliewer and H. Raether, J. Phys. C: Proc. Phys. Soc., London 7, 689 (1974).
[4]A. Mooradian, in *Laser Handbook*, edited by F. T. Arecchi and E. O. Schulz-DuBois (American Elsevier, New York, 1973).
[5]H. Lamvan, Diplomarbeit, Universität München, 1974 (unpublished).
[6]H. J. Höhberger, A. Otto, and E. Petri, Solid State Commun. 16, 175 (1975).
[7]C. J. Powell and J. B. Swan, Phys. Rev. 118, 640 (1960).
[8]R. H. Ritchie, Phys. Rev. 106, 874 (1957).
[9]N. W. Ashcroft and K. Sturm, Phys. Rev. B 3, 1898 (1971).
[10]D. Brust, Phys. Rev. B 2, 818 (1970).
[11]A. G. Mathewson and H. P. Myers, J. Phys. F: Metal Phys. 2, 403 (1972).
[12]A. Otto and W. Sohler, to be published.
[13]J. P. Walter and M. L. Cohen, Phys. Rev. B 5, 3101 (1972); M. S. Haque and K. L. Kliewer, Phys. Rev. B 7, 2416 (1973).
[14]S. G. Louie, J. R. Chelikowsky, and M. L. Cohen, Phys. Rev. Lett. 34, 155 (1975).
[15]H. J. Höhberger, dissertation, Universität München, 1974 (unpublished).
[16]H. Boersch, J. Geiger, A. Imbusch, and N. Niedrig, Phys. Lett. 22, 146 (1966).
[17]E-Ni Foo and J. J. Hopfield, Phys. Rev. 173, 635 (1968).
[18]T. Kloos, Z. Phys. 265, 225 (1973).
[19]O. von Roos and J. S. Zmuidzinas, Phys. Rev. 121, 941 (1961).
[20]P. Vashishta and K. S. Singwi, Phys. Rev. B 6, 875 (1972).
[21]L. W. Bos and D. W. Lynch, Phys. Rev. Lett. 25, 156 (1970).
[22]W. M. Saslow and G. F. Reiter, Phys. Rev. B 7, 2995 (1973).
[23]K. C. Pandey, P. M. Platzman, P. Eisenberger, and E-Ni Foo, Phys. Rev. B 9, 5046 (1974).
[24]E. Petri and A. Otto, to be published.
[25]P. M. Platzman and P. Eisenberger, Phys. Rev. Lett. 33, 152 (1974).

# Colored-Quark Version of Some Hadronic Puzzles

S. Nussinov
*Department of Physics and Astronomy, Tel Aviv University, Tel Aviv, Israel*
(Received 20 January 1975)

A simple picture based on colored quarks and gluons yields $\alpha_\rho(0)=\frac{1}{2}$, $\alpha_\Delta(0)=0$, and $\alpha_P(0)=1$, and explains various features of Pomeron exchange.

I adopt $SU(3)\otimes SU(3)'$ where strong interactions are mediated by $(\underline{1}\times\underline{8})$ colored gluons and hadrons are exact color singlet $q;\bar{q}$ $(\underline{3}\times\underline{3};\ \underline{3}^*\times\underline{3}^*)$ bound states.[1] A mechanism like the one of Casher, Kogut, and Susskind (CKS)[2] is assumed to generate spontaneous color neutralization which allows $e^+e^-\to$ hadrons at large $Q^2$ to be computed from the pointlike perturbation diagram. I suggest a generalization which may also provide a recipe for hadronic two-body, large-$s$, small-$t$ processes.

(i) The computation is first performed in the gluons quark basis. A transverse-momentum cutoff is introduced, hopefully making the CKS one-dimensional model more relevant. Ladder-type diagrams are naturally selected by the leading-logarithm approximation applicable to the cut-off theory.[3]